Technical Report No. 32-658

The Analysis of Uncooperative Radar Targets

R. M. Goldstein

JET PROPULSION LABORATORY
CALIFORNIA INSTITUTE OF TECHNOLOGY
PASADENA, CALIFORNIA

September 1, 1964

Technical Report No. 32-658

The Analysis of Uncooperative Radar Targets

R. M. Goldstein

M. Easterling, Chief
Communications Systems Research

JET PROPULSION LABORATORY
CALIFORNIA INSTITUTE OF TECHNOLOGY
PASADENA, CALIFORNIA

September 1, 1964

Prepared Under Contract No. NAS 7-100
National Aeronautics & Space Administration

CONTENTS

FIGURES

ABSTRACT

32998

By far the least cooperative class of targets that is likely to be accessible to radar is the group of our distant neighbors, the planets. This lack of cooperation stems from the all but incredible distances involved. However, when the modern high-power transmitter, large antenna, and ultrasensitive receiver are teamed together, these targets are detectable. In fact, echoes from Venus, Mars, Mercury, and Jupiter have been detected at JPL's DSIF station at Goldstone.

When the received power is large enough so that there is some margin left over from the requirements of straight detection, it becomes possible to gather much information about the target. Each point of the target has two attributes that can be measured independently at the receiver: its round-trip distance (or time delay), and its velocity (or doppler shift). Consider a rough, rotating planet as a target. All points which have the same time of flight lie on a circle, so that dividing the received power according to time delay is equivalent to dividing the target into concentric rings, centered about the sub-Earth point. All points which have the same doppler shift (due to rotational velocity) are found to project as straight lines parallel to the axis of rotation. Thus dividing the received power according to frequency shift is equivalent to dividing the target into parallel strips.

This paper discusses the special modulation and detection processes which enable the target to be analyzed into these two dimensions simultaneously. Such a system was used with Venus as the target during the conjunction of 1962, and a much improved version will be in operation for the conjunction of June 1964. It is expected that this system will yield very accurate measurements of the range of Venus, as well as the rotation rate, direction of the axis of rotation, and the detection of surface features on Venus.

Author

I. INTRODUCTION

As radar targets, the Moon and the planets are most uncooperative, a fact which stems from the tremendous distances involved. First contacts with such a target were made in 1946 and 1947, when a group from the U. S. Signal Corps (Ref. 1) and a group in Hungary (Ref. 2) succeeded in detecting radar echoes from the Moon.

A more difficult astronomical target is Venus; even at times of closest approach, it is 10 million times less cooperative than the Moon. Our technology required only 15 years of developing higher power transmitters, antennas of greater collecting area and focusing power, and more sensitive receivers in order to span this seven orders of magnitude. Radar contact with Venus was first made during the inferior conjunction of the spring of 1961 by four groups, working independently: JPL (Ref. 3) and MIT (Ref. 4) in the United States; Jodrell Bank (Ref. 5) in England, and a Crimean station (Ref. 6) in the USSR.

At the far point of its orbit, Venus becomes more difficult as a radar target by another factor of 1000. Our

technology has now covered this factor, and echoes have also been detected from Mars, Mercury, and Jupiter.

The basic task of radar astronomy is the analysis of such targets, i.e., the utilization of radar echoes to determine, insofar as is possible, the physical characteristics of the target planet. The greatest difficulty in accomplishing this task is the almost incredibly minute amount of power contained in a planetary echo. For example, the typical power density of a Venus echo, when that planet is at the far point of its orbit, is only 3×10^{-25} watts (0.2 photons per sec) per square meter. Because of background noise, which is eternally present, signal processing is a constant struggle to conserve signal-to-noise ratio.

II. TOTAL POWER

The measurement of power is fundamental to this task. If the signal is strong enough, more can be learned about the target if the echo power is divided according to its frequency content or according to its distribution in time. However, after such partitioning, the measurement reduces to the determination of the amount of power which remains in the selected "cell."

Total power measurements give directly the radar cross section of the target planet. Surface characteristics can be related to the cross section, and target motion and rotation can be related to time variation and periodicities of the cross section.

Power is defined as the average of the square of signal, so a natural method of power measurement follows this definition. Figure 1 is a block diagram of this method. The filter limits the amount of noise which is presented to the square law device.

The output w, on the average, equals the sum of the noise power through the filter w_n and the signal power w_s

$$\bar{w} = w_s + w_n \tag{1}$$

where the bar denotes ensemble average. Because of the random nature of the signal and the noise, w varies about its average value with a standard deviation of σ_w.

$$\sigma_w^2 = \bar{w}^2 - \bar{w}^2$$

A performance criterion SNR (or postdetection signal-to-noise ratio) is

$$\text{SNR} = w_s/\sigma_w \tag{2}$$

The design problem is to make SNR as large as possible. The following equations hold:

$$u(t) = \int_{-\infty}^{\infty} h(x)\,[s(t-x) + n(t-x)]\,dx$$

$$v(t) = u^2(t)$$

$$w = \frac{1}{T}\int_0^T v(t)\,dt$$

It can be shown that, in order to maximize SNR, $H(f)$ must be chosen such that

$$|H(f)|^2 = S_s(f) \tag{3}$$

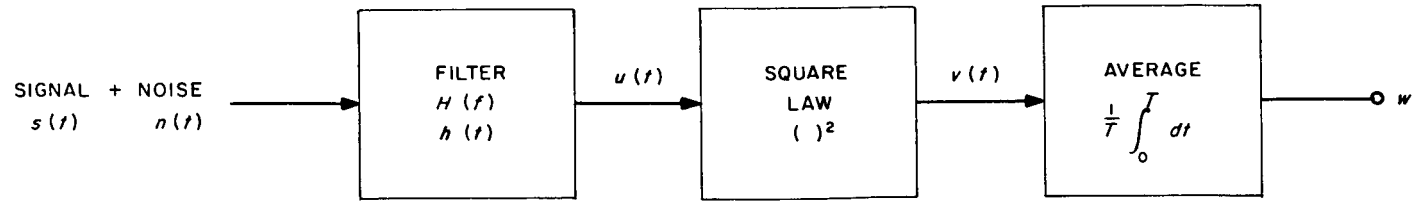

Fig. 1. Power meter block diagram

where $S_s(f)$ is the power spectral density of the signal, and the noise has been assumed white. It can also be shown that, under the assumption of white Gaussian noise, the block diagram of Fig. 1 results in an optimum power meter (radiometer). When $H(f)$ is properly chosen, the SNR that results is

$$\text{SNR} = \frac{1}{N}\sqrt{T\int_0^\infty S_s^2(f)\,df} \tag{4}$$

where T is the integration (observation) time and N is the noise spectral density (one-sided).

Equation (4) contains two inexorable laws of radar: for a given signal power, those signals which have larger $\int S_s^2(f)df$ (i.e., narrow-band signals) are more easily detected, and a factor of k loss in signal power can be compensated for by a factor of k^2 increase in observation time.

There are two difficulties in applying Eqs. (3) and (4) to a practical situation. First is the fact that $S_s(f)$ is usually unknown. Indeed, it may well be the quantity we set out to measure. Therefore, it is often assumed that $S_s(f)$ is a rectangular function of some bandwidth B. Of course, a search problem exists in the case of the weaker signals. They may not be detectable at all unless the proper bandwidth is utilized.

When such an $S_s(f)$ is substituted into Eq. (4), it becomes

$$\text{SNR} = \frac{w_s}{N}\sqrt{\frac{T}{B}} \tag{6}$$

which is the well-known radiometer formula.

The second difficulty is the problem of resolving w into its two parts, w_s and w_n. There are always troublesome gain variations in a practical system which make this separation difficult. One common method of solving this problem is to key the signal on and off (easily done at the transmitter) and identify w_s with the *change* in w. Thus the measurement is independent (to first order) of varying system gain. Of course, this technique reduces SNR somewhat,

$$\text{SNR} = \frac{w_s}{2N}\sqrt{\frac{T}{B}} \tag{7}$$

Equation (7) is known as the switched radiometer formula, and the factor of ½ is the cost of that practical consideration.

III. POWER DISTRIBUTION IN FREQUENCY

When the received signal contains more power than the requirements of pure detection, it becomes possible to learn much more about the characteristics of the target planet by measuring the power spectrum of the echo. For this measurement a spectrally pure sine wave is transmitted. The echo is both shifted and broadened in frequency by the doppler effect. The shift is caused by the relative orbital velocity between the planet and the radar station. Measurements of this shift have been used to compute the astronomical unit (Ref. 7) and will be used to improve the Venus and Earth ephemerides.

The doppler broadening is caused by any apparent rotation the planet may have, since different parts of the surface will have different line-of-sight velocities. Rotation has two components: one is the normal spin about an axis, and the other is the relative orbital motion, which also produces doppler broadening. The situation is illustrated in Fig. 2, where the contours of constant line-of-sight velocity (and hence frequency shift) have been drawn. These contours are circles, such that they appear to the radar station as equispaced lines, all parallel to the projected axis of rotation.

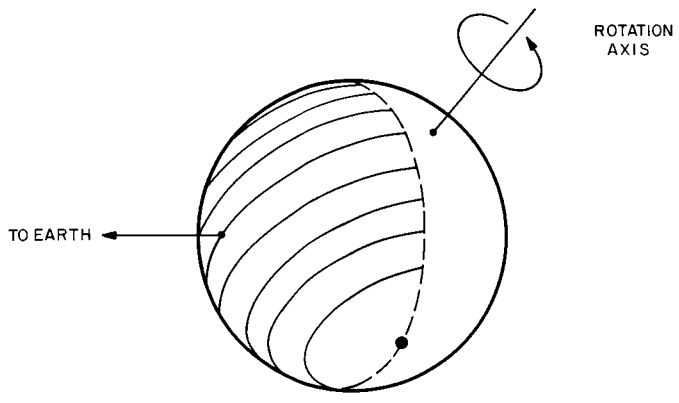

Fig. 2. Contours of constant frequency shift

Thus a spectrogram of the echo power is equivalent to scanning the disk with a narrow slit parallel to the contours of Fig. 2. The amount of frequency broadening B, corresponding to reflections from the extreme contours, is

$$B = \frac{4\,\Omega\, r}{\lambda} \tag{8}$$

where Ω is the projected rotation rate, r is the radius, and λ is the wavelength. Observations of Venus during the conjunction of the fall of 1962 (Ref. 8) produced the surprising results showing that Venus rotates *retrograde,* with a period of about 250 days.

Inferences about the scattering properties of the surface can be made, based upon the shape of the spectrum. For example, if the surface is smooth, most of the power will be returned from the sub-Earth area, and the spectrum will be highly peaked. Figure 3 is a sample spectrogram taken of Venus at a distance of 88 million miles from Earth. To be quantitative, we define the backscatter function $F(\theta)$ to be the radar cross section of a unit area of surface, taken as a function of the angle of incidence. Figure 4 illustrates this point.

Given $F(\theta)$ and the assumptions of a homogeneous surface (all elements of the sphere have the same $F(\theta)$), and a surface such that the power from individual elements adds, then the signal spectrum $S_s(f)$ can be computed as

$$S_s(f) = \int_{\sin^{-1} f/a}^{\pi/2} \frac{F(\theta)\sin\theta\, d\theta}{(a^2\sin^2\theta - f^2)^{1/2}} \tag{9}$$

where a is a rotation constant.

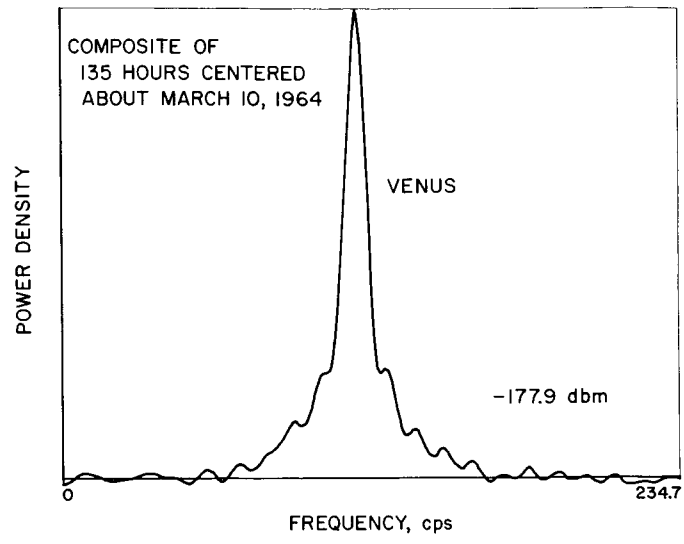

Fig. 3. Venus spectrogram

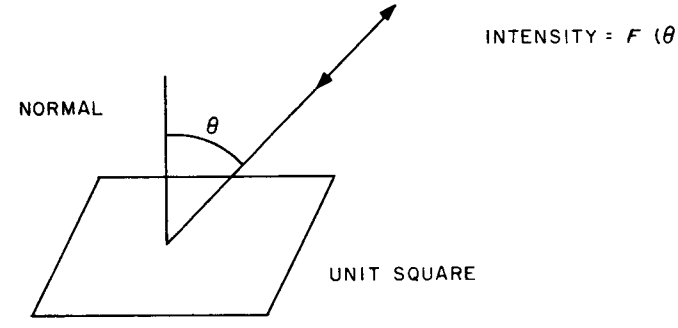

Fig. 4. Backscatter function

Equation (9) shows the dependence of $S_s(f)$ upon $F(\theta)$. This equation has been inverted to yield

$$F(\theta) = -\frac{2a^2\cos\theta}{\pi}\int_{a\sin\theta}^{a} \frac{S'(f)\, df}{(f^2 - a^2\sin^2\theta)^{1/2}} \tag{10}$$

Equations (9) and (10) form a transform pair. Thus measurement of the spectrum of the echo reveals the backscattering characteristic of the surface.

In radar astronomy, transmission is normally circularly polarized. A single reflection reverses the sense of circular polarization, so the receiver is usually set to receive the opposite sense. However, if the surface is rough compared to the size of the wavelength, double reflections will occur. If the transmitter and receiver are both

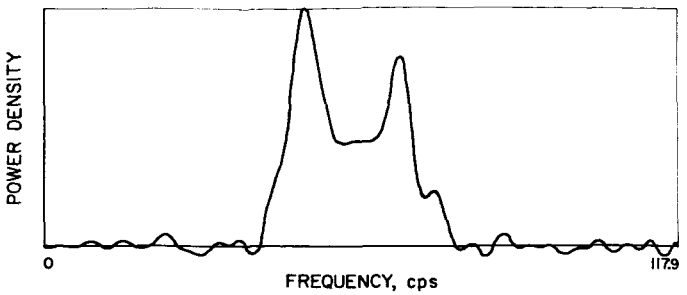

Fig. 5. Cross-polarized Venus spectrogram, June 27, 1964

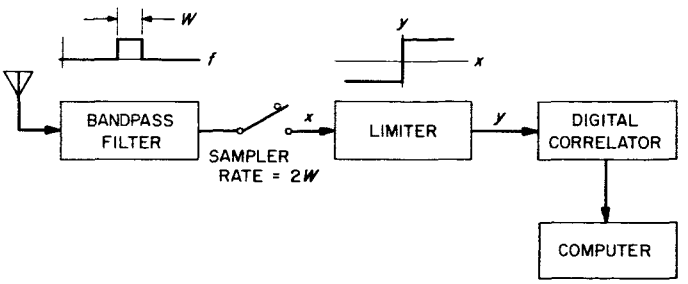

Fig. 6. Spectrometer block diagram

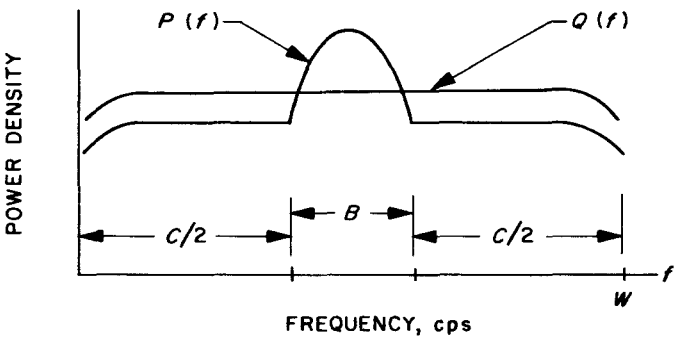

Fig. 7. Signal-plus-noise and noise-only spectra

circularly polarized in the same sense, only double reflections (or any *even* number) will be received. Figure 5 is a sample spectrogram taken of Venus in the light of double reflections only.

The total power in this mode is less by a factor of about 18 (for Venus), but interesting features are revealed. The very strong central spike is missing and certain rough areas of Venus are clearly seen. As Venus rotates, these areas move slowly across the spectrograms, from the high-frequency side to the low.

The spectrograms shown in the figures were made by the autocorrelation approach (Ref. 9). Figure 6 is a block diagram of the system. The maser, programmable local oscillator, and several stages of IF amplification and conversion, etc., are all labelled BANDPASS FILTER. Samples x_i of the signal are taken at the Nyquist rate. They are quantized to only two levels by the limiter. The correlator forms the following sums of the quantized signal y_i:

$$R_y(k) = \frac{1}{I} \sum_{i=1}^{I} y_i\, y_{i+k} \qquad k = 1, 2, \cdots, K \qquad (11)$$

where $R_y(k)$ is the estimate of the autocorrelation function of the signal at y. Two-level quantization is done to make the sums of Eq. (11) easy to mechanize. The y_i always equal ± 1, and multiplication and addition are greatly simplified.

One might expect the action of the limiter to alter the spectrum beyond recovery; but fortunately this is not so, and a simple formula relates the autocorrelation function at y to that at x.

$$R_x(k) = R_x(0) \sin\left[\frac{\pi}{2} R_y(k)\right] \qquad (12)$$

This correction is made by the computer, which then calculates the spectrum by:

$$S(f) = 2 \sum_{k=1}^{K} R_x(k) \cos(\pi k f/W) + 1 \qquad (13)$$

It can be shown that this method is equivalent in performance to a set of stagger-tuned, optimum radiometers, except for a factor of $2/\pi$. That is the cost in performance of the simplification allowed by use of only two-level quantization.

In practice, a measured spectrum is always the sum of the signal spectrum plus the noise spectrum. It is desirable not only to subtract off the noise spectrum but to estimate the total power as well in order to provide a measurement of the radar cross section. The raw material for this is two spectra: $P(f)$, the sum of signal plus noise, and $Q(f)$, the noise only. Typical spectra such as these are illustrated in Fig. 7. They have been normalized to unit power to remove the problem of system gain variations.

$$P(f) = \frac{S_s(f) + S_n(f)}{w_s + w_n}$$

$$Q(f) = \frac{S_n(f)}{w_n} \qquad (14)$$

A good estimate $W(f)$ of the signal spectrum is

$$W(f) = P(f) - kQ(f) \tag{15}$$

where k is a constant to be determined. If k is properly chosen, the average of $W(f)$ over the frequency interval C (where there the signal component is known to be zero) would be zero. This condition defines k:

$$k = \frac{\int_C P(f)\,df}{\int_C Q(f)\,df} \tag{16}$$

It can be seen, from Eqs. (14) and (16) that

$$w_s = w_n \frac{1-k}{k} \tag{17}$$

The performance criterion SNR of this method of determining the total power is

$$\text{SNR} = \frac{w_s}{N}\sqrt{\frac{CT}{2(W-C)\,W}} \tag{18}$$

where W is the total spectrometer bandwidth. Equation (18), for $C = W/2 = B$, the signal bandwidth, is exactly the switched radiometer formula (Eq. 7).

In the limit as $C = W - B$ and $W \to \infty$ (of course, the spectrometer complexity increases), Eq. (18) becomes

$$\text{SNR} = \frac{w_s}{N}\sqrt{\frac{T}{2B}} \tag{19}$$

It must be noted that measuring $P(f)$ and $Q(f)$ requires twice as much time as measuring $P(f)$ only: but, in the monostatic radar case, this time is available while the transmitter is on.

IV. POWER DISTRIBUTION IN RANGE

Range measurement is essentially a problem of estimation of time delay. A modulated signal is transmitted, and the time required for the signal to return is a direct measure of the distance.

Detection theory tells us that (under some simplifying assumption) the best way to estimate time delay is to compare, by correlation, the signal with the possible expected signals, of various time delay. The closest comparison corresponds to the best estimate of time delay. Even where the simplifying assumptions are not strictly met, it is always good strategy to compare the actual signal with the possible expected ones.

Figure 8 is a block diagram of this method. Amplitude modulation is considered here; but frequency, single sideband, etc., modulation may be and has been used successfully. The performance of this system depends critically on the waveform chosen for $C(t)$. The ability of the system to distinguish between different range zones (or time delays) depends on the autocorrelation function $R(\tau)$ of $C(t)$, defined by

$$R(\tau) = \text{average}\,[C(t)\,C(t+\tau)]$$

For a time-of-flight (range) resolution of τ_0, $R(\tau)$ must be a highly peaked function for $|\tau| < \tau_0$. To eliminate "cross-talk" between range zones, $R(\tau)$ should be near zero for $|\tau| > \tau_0$.

Two commonly used $C(t)$ and their autocorrelation functions are given in Fig. 9. The first waveform, $C_1(t)$, is a high, narrow pulse; the second, $C_2(t)$, is a random square wave, such that after each time interval of τ_0, a random choice is made as to whether $C_2(t) = \pm 1$ for the next interval. Both of these waveforms have the same autocorrelation function and the same range resolution, but they lead to entirely different radar hardware; $C_1(t)$ leads to a pulse radar, with its energy concentrated into narrow pulses, and $C_2(t)$ leads to a CW radar, with constant power over a cycle.

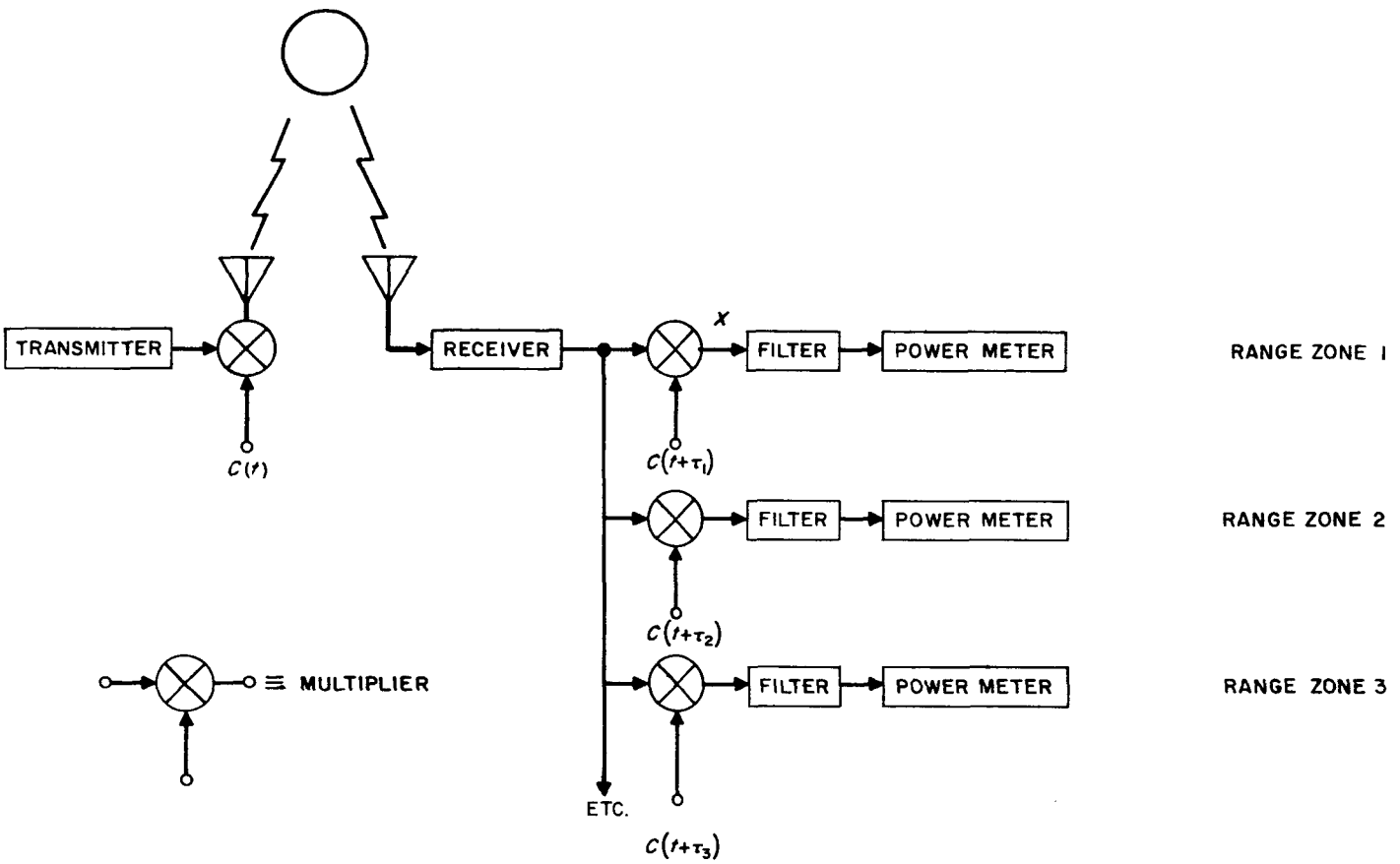

Fig. 8. Range-gate block diagram

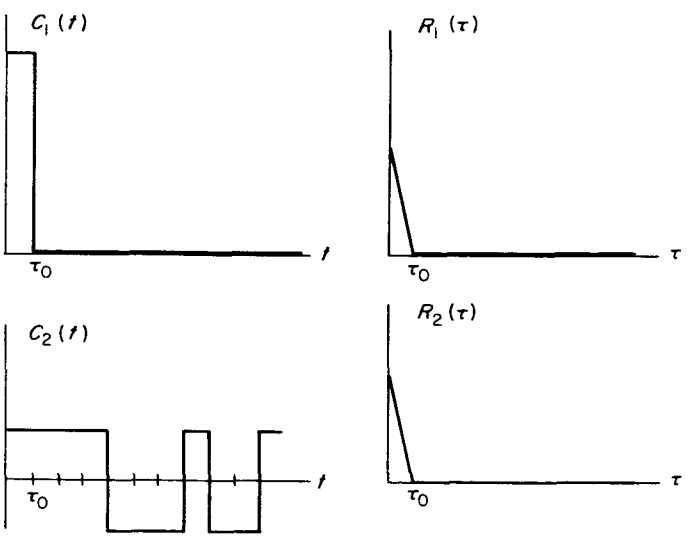

Fig. 9. Modulation waveforms and their autocorrelation function

Consider for the following discussion that the target is a perfect mirror, so that the received signal is only shifted in time, and attenuated, from the transmitted signal. This restriction will be removed subsequently when we consider range-velocity mapping. The signal spectra at point x of Fig. 8 are given in Fig. 10a for the "correct" range zone, i.e., for the zone which contains the signal.

The pulse radar produces a line spectrum, so that the optimum filter for the power meter is a "comb" filter, which allows the lines to pass through, but blocks as much of the noise as possible. The spectrum for the CW radar is a single impulse. The multiplier at the receiver serves to cancel, exactly, the modulation impressed upon the signal at the transmitter. Thus the signal is restored to a single sine wave. The optimum filter for this case is a narrow bandpass filter. There will be no signal spectrum in the "incorrect" range zones of the

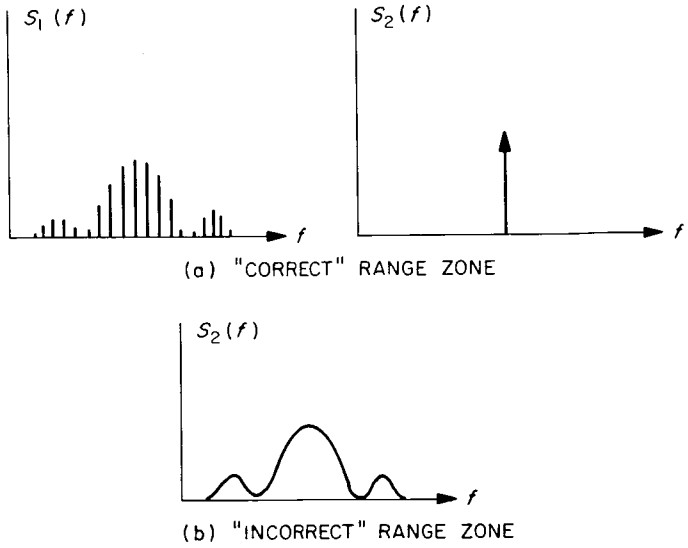

Fig. 10. Range-gated spectra, point target

pulse radar, only noise. The corresponding spectrum for the CW case is given in Fig. 10b. It is still wide-band, so it is largely eliminated by the narrow-band filter. The remainder is, in practice, negligible when compared to the ever-present noise. It is interesting to note that for the same *average* power transmitted, $C_1(t)$ and $C_2(t)$ lead to radars of the same performance in estimating range.

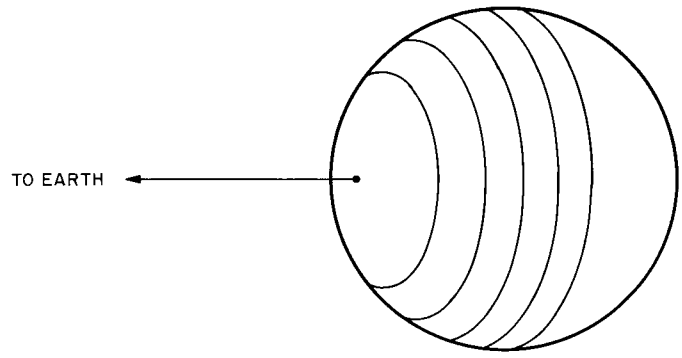

Fig. 11. Contours of constant range

Thus the set of range-gates divides the signal power according to its range composition. The contours of constant range are, of course, concentric circles centered about the sub-Earth point, as is illustrated in Fig. 11.

V. RANGE–VELOCITY MAPPING

The techniques of range-gating and spectral analysis may be combined simultaneously to produce a two-dimensional map of the surface of the target planet. The coordinates of such a map are along the contours of constant frequency shift and along the contours of constant range. Figure 12 illustrates this coordinate system. This system has an essential ambiguity, however, since there are, in general, two points on the planetary surface which have the same range and same line-of-sight velocity. This ambiguity may be resolved by observing the target planet at different times, when the rotation axis makes different angles to the line of sight.

The mechanization of this scheme, for the CW radar, is the same as for the range gates of Fig. 8, except that the power meters are replaced by spectrometers. A simi-

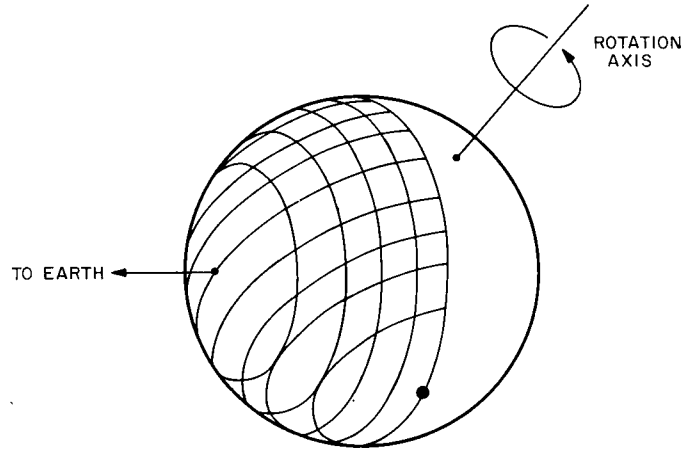

Fig. 12. Contours of constant range and constant frequency shift

lar mechanization (Ref. 10) can be used for the pulse-radar case. Each range-gate responds to only that echo which originates from the selected range zone and restores that signal to its sine wave form. The frequency of that sine wave depends, of course, on the line-of-sight velocity of the reflecting surface element. When this echo is resolved into its frequency spectrum, the two-dimensional mapping process is completed.

The theoretical limit of resolution in the range dimension and, simultaneously, in the frequency dimension is limited only by the stability of the oscillators of the system. In practice, the resolution attainable is limited by the signal-to-noise ratio. As the echo power is divided into smaller and smaller "cells," it finally cannot be distinguished from the background noise.

Figures 13 and 14 are actual samples of range-gated spectra of Venus echoes. Only the first few range zones near the sub-Earth point are shown. The spectra of all but the first few have the "double humped" shape characteristic of the coordinate system used and which stems from the oblique intersection of the coordinates near the frequency extremes. Any departures from this characteristic shape may be interpreted as features on the target's surface. As the planet rotates, permanent features will trace their signatures upon the spectra by moving from the high- to the low-frequency side, and, depending upon the feature's latitude, through the range zones.

Venusian features may be seen in Figs. 13 and 14. The peaks which appeared in zones 2 and 3 on June 13, 1964, had moved to become peaks in zones 4 and 5 by June 27, 1964.

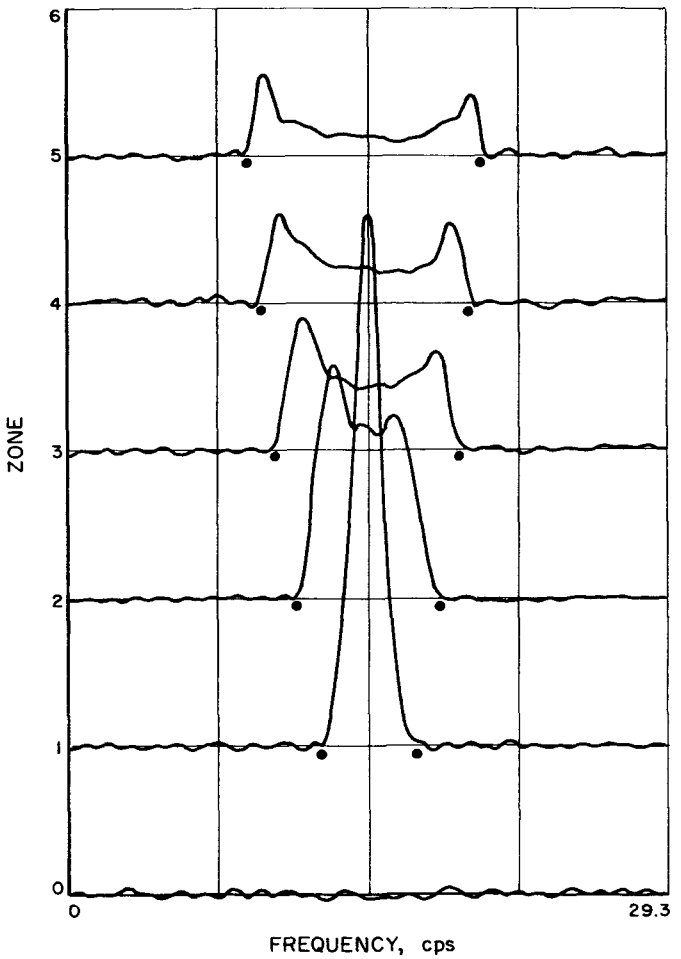

Fig. 13. Range-gated Venus spectra, June 13, 1964, 46-mile zones

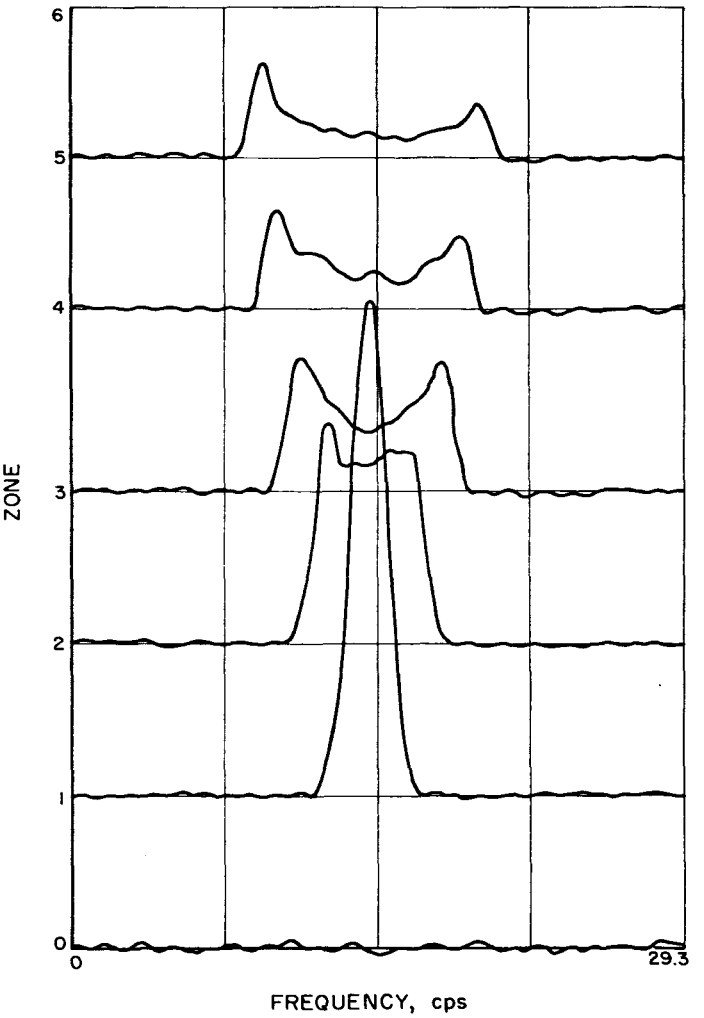

Fig. 14. Range-gated Venus spectra, June 27, 1964, 46-mile zones

The base bandwidths of the spectra (i.e., the frequency interval corresponding to the extreme frequency contours for the given range zone), measured over a time interval of several months, may be used to determine the rotation period of Venus and the direction in space of the axis. The bandwidths predicted from the JPL observations of 1962 (250 days retrograde) have been plotted on the figures.

The round-trip time-of-flight can be measured from these spectra with surprising precision by noting the positions and widths of the echoes in the range zones.

For example, at 24:00 GMT, June 13, the time-of-flight was 294.17890 $\pm$.00012 sec. Measurements made with 11-mile range-gates have yielded a precision of $\pm$.00003 sec.

REFERENCES

1. DeWitt, J. H., Jr., and Stodola, E. K., "Detection of Radio Signals Reflected from the Moon," *Proc. IRE*, Vol. 37, No. 3, pp. 229–242, March 1949.
2. Bay, Z., *Hung. Acta Phys.*, Vol. 1, No. 1, 1946.
3. Victor, W., Stevens, R., and Golomb, S., *Radar Exploration of Venus*, Technical Report No. 32-132, Jet Propulsion Laboratory, Pasadena, August 1961.
4. Pettengill, G. H., et al, "A Radar Investigation of Venus," *Astron. J.*, Vol. 67, pp. 181–190, May 1962.
5. Thomson, J. H., et al, "A New Determination of the Solar Parallax by Means of Radar Echoes from Venus," *Nature*, Vol. 190, No. 4775, p. 519, May 6, 1961.
6. Kotelnikov, V. A., "Radar Contact with Venus," *Brit. J. IRE*, Vol. 22, No. 4, pp. 293–295, October 1961.
7. Muhleman, D. O., et al, "The Astronomical Unit Determined by Radar Reflections from Venus," *Astron. J.*, Vol. 67, No. 4, May 1962.
8. Goldstein, R. M., and Carpenter, R. L., "Rotation of Venus: Period Estimated from Radar Measurements," *Science*, Vol. 139, No. 3558, pp. 910–911, March 8, 1963.
9. Blackman, R. R., and Tukey, J. W., *The Measurement of Power Spectra*, Dover Publ., Inc., New York, N. Y., 1958.
10. Pettengill, G. H., "Radio Frequency Scattering from the Surface of the Moon," *Proc. IRE*, Vol. 48, pp. 932–934, 1960.

ACKNOWLEDGMENT

The author gratefully acknowledges the work of R. L. Carpenter and D. O. Muhleman, who have been his colleagues throughout the radar experiments, and H. C. Rumsey, who inverted the integral of Eq. (9).